Radiochim. Acta **90**, 1–5 (2002)

Cross section data for the production of the positron emitting niobium isotope ^{90}Nb *via* the ^{90}Zr(*p*, *n*)-reaction

By S. Busse[1,2], F. Rösch[1,*] and S. M. Qaim[2]

[1] Institut für Kernchemie, Johannes Gutenberg-Universität, D-55128 Mainz, Germany
[2] Institut für Nuklearchemie, Forschungszentrum Jülich GmbH, D-52425 Jülich, Germany

(Received April 19, 2001; accepted in revised form July 16, 2001)

Positron emitter ^{90}Nb */ Nuclear reaction / Excitation function / Calculated integral yield / Experimental thick target yield / Radionuclidic impurities*

Summary. The radioisotope ^{90}Nb decays with a positron branching of 53% and a relatively low β^+-energy of $E_{mean} = 0.66$ MeV and $E_{max} = 1.5$ MeV. Its half-life of 14.6 h makes it especially promising for quantitative investigation of biological processes with slow distribution kinetics using positron emission tomography. To optimise its production, the excitation functions of ^{90}Zr(p, xn)-processes were studied over the proton energy range of 7.5 to 19 MeV *via* the stacked-foil technique using both ^{nat}Zr and 99.22% enriched $^{90}ZrO_2$ as targets. Thick target yields of ^{90}Nb were calculated from the measured excitation functions and were verified experimentally. The optimum energy range for the production of ^{90}Nb *via* the ^{90}Zr(p, n)-process was found to be $E_p = 17 \rightarrow 7$ MeV, with a yield of 600 MBq ^{90}Nb/μA h. The yield and radionuclidic purity of ^{90}Nb over the energy range of $E_p = 17.6 \rightarrow 8.1$ MeV were determined experimentally using ^{nat}Zr. At 4 h after EOB the yield of ^{90}Nb was found to be 290 MBq/μA h and its radionuclidic purity ≥ 95%.

Introduction

The radioisotope ^{90}Nb is a positron emitter with a positron branching of 53% and a relatively low β^+-energy of $E_{mean} = 0.66$ MeV and $E_{max} = 1.5$ MeV. Its half-life of 14.6 h renders it especially promising for quantitative investigation of slow biological processes, in particular those involving labeled peptides and proteins, *via* positron emission tomography. Recently, the radiochemical separation of no-carrier-added ^{90}Nb from macroscopic zirconium targets and first approaches to introduce no-carrier-added ^{90}Nb into peptidic tracers such as the octreotide derivative DFO-succinyl-(D)Phe^1-octreotide (SDZ 216-927) using the bifunctional ligand desferrioxamine have been described [1, 2].

^{90}Nb was originally identified *via* the (d, $2n$) reaction on ^{90}Zr [3]. High-purity ^{90}Nb was first obtained *via* the ^{93}Nb(p, $4n$)^{90}Mo → ^{90}Nb process [4]. For the production of ^{90}Nb today, several nuclear reactions seem to be reasonable: the (p, n)- or (d, $2n$)-process on ^{90}Zr and the (^{3}He,$2n$)- or (α, $3n$)-reactions on natural yttrium. A medium-sized cyclotron would allow the production of ^{90}Nb *via* the (p, n)-, (d, $2n$)- or the (^{3}He, $2n$)-process. In fact even a small-sized cyclotron ($E_p \leq 16$ MeV) should lead to sufficient quantities of the radioisotope *via* the (p, n)-reaction. A few studies have shown that the (d, $2n$)-reaction requires a deuteron energy of about 16 MeV [5–7], the (^{3}He, $2n$)-process a ^{3}He-energy of ≥ 30 MeV and the (α, $3n$)-reaction an α-particle energy of ≥ 45 MeV [8]. Furthermore, the systematics of (^{3}He, $2n$)- and (p, n)-reactions suggest that the production yield of ^{90}Nb should be higher in the latter process. With the common availability of dedicated cyclotrons for producing short-lived β^+-emitters, the (p, n)-reaction represents an advantageous route for production of ^{90}Nb. Some cross section data on the ^{nat}Zr(p, xn)-reactions using thick target irradiations with high initial proton energy have already been reported in the literature [9, 10]. However, those experiments were not designed to determine cross sections in the low energy region relevant to the production of ^{90}Nb, *i.e.* at $E_p < 20$ MeV. The data may have large errors because large foil-stacks with high incident proton energies (for example, $E_p = 70 \rightarrow 10$ MeV) were used.

The aim of this study was to investigate proton induced reactions on ^{nat}Zr and ^{90}Zr and to measure the experimental production yield and radionuclidic purity of the desired product.

Experimental

Cross sections were measured as a function of incident proton energy using the conventional stacked-foil technique, as described earlier, cf. [11, 12]. Thick target yields were determined using thicker targets. Some of the salient features of the present experiments are given below.

Target material

For irradiations with incident proton energies up to 15 MeV, *i.e.* the onset of the ^{91}Zr(p, $2n$)^{90}Nb-process, ^{nat}Zr was used as target material in the form of 10 μm or 250 μm thick foils. Commercially available ^{nat}Zr metal foils were used as supplied by Goodfellow Metals. The isotopic composition of natural Zr is: ^{90}Zr (51.45%), ^{91}Zr (11.32%), ^{92}Zr (17.19%),

*Author for correspondence (E-mail: frank.roesch@uni-mainz.de).

^{94}Zr (17.28%), ^{96}Zr (2.76%). The chemical purity was specified by the supplier as 99.8+%. The remaining typical impurities in ^{nat}Zr (in ppm) were: Nb (50), Hf (250), Fe (200), Cr (200), Al (40), Ti (20), Ni (20), Cu (20), V (20), W (200), rare earths (50).

For irradiations at proton energies above 12 MeV, isotopically enriched ^{90}Zr was used. To prepare ^{90}Zr samples commercially available metal dioxide powder from Campro Scientific was used. The isotopic composition in this case was: ^{90}Zr (99.22%), ^{91}Zr (0.39%), ^{92}Zr (0.29%), ^{94}Zr (0.15%), ^{96}Zr (0.01%). The content of impurities (in ppm) was specified as: Fe (50), Cr (60), Al (30), Ti (20), Ni (< 20), Cu (50).

Sample preparation

In the case of ^{nat}Zr, samples for cross section measurements were prepared by cutting pieces of 13 mm diameter out of a 10 μm thick metal foil. For thick target yield measurements, discs of 250 μm thickness were cut out of a large-sized metal foil.

Thin samples of enriched ^{90}Zr were prepared by means of a special sedimentation technique. Details of this procedure were described in [13]. In brief, a suspension of 5–6 mg of very fine $^{90}ZrO_2$ powder in 100 μl of water-free chloroform in an Eppendorf vessel was prepared by action of an ultrasonic bath for 3 min. The suspension was transferred to a cylindrical polytetrafluoroethylene (PTFE) vessel (10 mm diameter) with a 13 mm diameter copper foil (25 μm thick) as removable bottom. The chloroform of the suspension was allowed to evaporate slowly. The copper foil and the empty PTFE cylinder were then carefully separated from each other. A homogeneous and mechanically stable $^{90}ZrO_2$ sample of thickness in the order of 5–6 mg/cm^2 was thus obtained on the surface of the copper backing foil. To provide mechanical stability to the sedimented layers a thin adhesive polymer film (< 1 mg/cm^2) was sprayed over the samples. Furthermore, to avoid contamination, the surface of each sample was covered with a 10 μm thick Al foil, having the same diameter of 13 mm as the Cu backing foil.

Irradiations and beam current monitoring

For cross section measurements, several stacks, each containing five or six ^{nat}Zr foils or six $^{90}ZrO_2$ sedimented samples, were irradiated at the Jülich compact cyclotron CV 28, each for 30 min at a beam current of 100 nA. The primary proton energies used were 20, 16 and 12 MeV. For the measurement of thick target yields and isotopic impurities a 30 min irradiation at 1 μA was carried out using a stack of three 13 mm ∅ ^{nat}Zr foils, each 250 μm thick. Each stack contained a Cu monitor foil (25 μm thick) on the front side. For incident proton energies > 14 MeV, it was thus possible to control the proton energy experimentally *via* the energy dependent ratio $\sigma_{(p,2n)}/\sigma_{(p,n)}$ of the monitor reactions ^{63}Cu$(p,2n)^{62}$Zn and ^{63}Cu$(p,n)^{63}$Zn, cf. [14]. The proton beam current was measured directly using a Faraday cup as well as indirectly *via* the ^{63}Cu$(p,n)^{63}$Zn reaction, cf. [15]. At low intensities the proton flux measured *via* the two techniques differed considerably. We therefore put more reliance on the monitor reaction.

Measurement of radioactivity

The absolute radioactivity was determined by γ-ray spectrometry using either a Ge(Li) or a HPGe detector coupled to an Ortec (Spectrum ACE) 4 K MCA plug-in card. The card was connected to an IBM-compatible PC-AT. The peak area analysis was done using the software Gamma Vision® 4.10. The detector counting efficiencies for different photon energies and counting distances were determined using calibrated standard sources (errors $< 3\%$) obtained from PTB Braunschweig and Amersham International.

The radioactivity was measured non-destructively, *i.e.* the ^{90}Zr samples on Cu backing foils together with the Al covers were counted without a mechanical removal of the covering foil or chemical treatment of the target material. With respect to cross section measurements, counting was performed only over two days after each irradiation, and attention was paid exclusively to the short-lived Nb isotopes ^{90}Nb, ^{89}Nb and ^{89m}Nb. Apart from the activity of the mentioned isotopes the activity of the monitor reaction products ^{62}Zn and ^{63}Zn was also determined. The decay data used in the γ-ray spectroscopic analysis of the radioisotopes investigated were taken from Ref. [16] and are summarized in Table 1.

Calculation of cross sections and errors

The count rates were corrected for pile-up losses as well as for γ-ray intensities and the efficiencies of the detectors. The uncertainties due to random coincidences were kept small by choosing a sample to detector distance such that the dead time was $< 7\%$. Since the distance between the sample and the detector was always > 10 cm, the correction for real coincidence losses was negligible. The cross sections were calculated using the well-known activation formula. The overall uncertainty in each cross section was obtained by taking the square root of the sum of the squares of the individual uncertainties, which were considered to be as follows:

- target mass ($\sim 2\%$),
- inhomogeneity in target thickness (5%–10%),

Table 1. Decay data of the product nuclei used in the present study, cf. [16].

Nuclide	Mode of decay (%)	$T_{1/2}$	E_γ [keV]	γ-abundance [%]
^{89m}Nb	β^+ (81)	66.0 min	588.0	99.5
	EC (19)		507.4	85.0
^{89}Nb	β^+ (75)	2.0 h	1833.4	3.2
	EC (25)		1627.0	3.0
			920.5	1.4
^{90m}Nb	IT (100)	18.8 s	122.4	64.2
^{90}Nb	β^+ (53)	14.6 h	1129.1	92.0
	EC (47)		2319.1	82.8
			141.2	69.0
^{63}Zn	β^+ (93)	38.1 min	669.8	8.4
	EC (7)		962.6	6.6
^{62}Zn	EC (93.1)	9.23 h	548.4	15.2
	β^+ (6.9)		596.7	25.7

- statistical errors (2%–10%; for energy points near the threshold up to 20%),
- detector efficiency and sample-detector geometry ($\sim$ 6%),
- decay data errors ($<$ 3%),
- bombarding proton beam intensity (8%–10%).

For the ^{90}Zr(p, n)-reaction the overall error in cross section amounts to 15 to 20%. The primary proton energy had an error of $\pm$0.2 MeV. The proton energy degradation in each stack foil or $^{90}ZrO_2$ sample was calculated and its half-value was combined with the uncertainty of the primary energy. The uncertainty in the effective energy of the front foil was estimated to be 0.3 MeV. Due to propagation of error it increased to 0.7 MeV in the sixth foil of a stack.

Results and discussion

Cross section data

The measured cross sections of the ^{90}Zr(p, n)^{90}Nb, ^{90}Zr (p, 2n)^{89m}Nb and ^{90}Zr(p, 2n)^{89}Nb reactions are given in Table 2. The data for ^{90}Nb describe the cumulative formation cross sections of the 14.6 h isotope, since the 18.8 s isomeric state ^{90m}Nb decays 100% by IT to ^{90}Nb. Because of the short half-life of ^{90m}Nb, a short cooling time of only a couple of minutes was sufficient to allow complete decay of ^{90m}Nb before the γ-ray measurements. The data given for ^{89m}Nb and ^{89}Nb describe the direct production cross sections, *i.e.* without involving the decay of any precursor.

Detailed cross sections of the ^{90}Zr(p, n)^{90}Nb-reaction over the most relevant proton energy region of 7.5 to 19 MeV have been measured for the first time in this work. Up to 15 MeV, ^{nat}Zr was used as target material, and correction for isotopic composition was made. Beyond 15 MeV, use of enriched ^{90}Zr was necessary, because of increasing contribution of the ^{91}Zr(p, 2n)-process to the formation of ^{90}Nb. Between 12 and 15 MeV, a few measurements were carried out using both ^{nat}Zr and ^{90}Zr to check the consistency of results.

Our cross section data are shown as a function of proton energy in Fig. 1 together with the results of an earlier study [9]. The ^{90}Zr(p, n)-reaction leading to the formation of ^{90}Nb has a threshold of about 7 MeV and reaches a maximum cross section of about 820 mb at 13.5 MeV. These results show considerable deviations from the data reported by Kondratev *et al*. [9], who gave a maximum cross section of 661 mb at a somewhat higher energy of about 17 MeV. However, as mentioned above, those experiments were not designed to measure accurate cross sections in the low energy region. Considering the (p, n)-excitation functions for some other target nuclei in this mass region investigated in recent years, *e.g.* ^{85}Rb [17], ^{86}Sr [13] and ^{94}Mo [18], our data appear to be more precise than the values given in Ref. [9].

At proton energies higher than 17 MeV the ^{90}Zr(p, 2n)-process also occurs, leading to the isotopes ^{89m}Nb and ^{89}Nb. Those results are also shown in Fig. 1.

Table 2. Cross sections for the formation of ^{90}Nb, ^{89m}Nb and ^{89}Nb in proton induced nuclear reactions on ^{nat}Zr and on highly-enriched ^{90}Zr.

Target material	Thickness [mg/cm^2]	E_p [MeV]	^{nat}Zr	$^{90}ZrO_2$		
			$\sigma(^{90}Nb)^a$ [mb]	$\sigma(^{90}Nb)^a$ [mb]	$\sigma(^{89m}Nb)^b$ [mb]	$\sigma(^{89m}Nb)^b$ [mb]
$^{90}ZrO_2$	5.9	19.0 $\pm$ 0.3	–	243 $\pm$ 41	67 $\pm$ 15	91 $\pm$ 40
$^{90}ZrO_2$	5.6	18.4 $\pm$ 0.3	–	271 $\pm$ 43	43 $\pm$ 10	64 $\pm$ 32
$^{90}ZrO_2$	5.6	17.8 $\pm$ 0.3	–	352 $\pm$ 63	23 $\pm$ 6	43 $\pm$ 26
$^{90}ZrO_2$	5.0	17.2 $\pm$ 0.3	–	460 $\pm$ 86	9 $\pm$ 3	
$^{90}ZrO_2$	5.5	16.6 $\pm$ 0.3	–	556 $\pm$ 93		
$^{90}ZrO_2$	5.7	16.0 $\pm$ 0.3	–	617 $\pm$ 98		
$^{90}ZrO_2$	5.9	15.5 $\pm$ 0.3	–	743 $\pm$ 111		
^{nat}Zr	7.5	15.3 $\pm$ 0.3	859 $\pm$ 123	–		
$^{90}ZrO_2$	5.6	14.9 $\pm$ 0.3	–	791 $\pm$ 144		
^{nat}Zr	7.2	14.3 $\pm$ 0.4	816 $\pm$ 148	–		
$^{90}ZrO_2$	5.6	14.2 $\pm$ 0.4	–	771 $\pm$ 125		
$^{90}ZrO_2$	5.0	13.5 $\pm$ 0.3		876 $\pm$ 152		
^{nat}Zr	7.2	13.5 $\pm$ 0.4	797 $\pm$ 125			
^{nat}Zr	7.5	13.2 $\pm$ 0.4	809 $\pm$ 121			
$^{90}ZrO_2$	5.5	12.8 $\pm$ 0.4	–	826 $\pm$ 132		
^{nat}Zr	7.2	12.6 $\pm$ 0.5	749 $\pm$ 137			
^{nat}Zr	7.2	12.3 $\pm$ 0.4	763 $\pm$ 131			
$^{90}ZrO_2$	5.6	12.0 $\pm$ 0.6	–	808 $\pm$ 125		
^{nat}Zr	7.1	11.6 $\pm$ 0.6	728 $\pm$ 111			
^{nat}Zr	7.2	11.3 $\pm$ 0.4	724 $\pm$ 129			
^{nat}Zr	7.6	11.1 $\pm$ 0.3	640 $\pm$ 115			
^{nat}Zr	7.2	10.6 $\pm$ 0.7	647 $\pm$ 110			
^{nat}Zr	7.2	10.3 $\pm$ 0.5	650 $\pm$ 127			
^{nat}Zr	7.6	10.0 $\pm$ 0.4	590 $\pm$ 105			
^{nat}Zr	7.1	9.1 $\pm$ 0.6	524 $\pm$ 95			
^{nat}Zr	7.4	8.8 $\pm$ 0.4	408 $\pm$ 105			
^{nat}Zr	7.2	7.9 $\pm$ 0.7	292 $\pm$ 70			
^{nat}Zr	7.5	7.5 $\pm$ 0.5	132 $\pm$ 31			

a: Cumulative cross section
b: Independent formation cross section

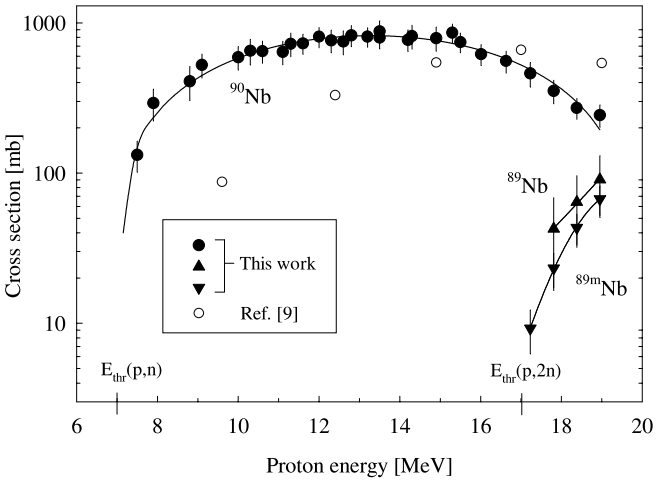

Fig. 1. Excitation functions of ^{90}Zr(p, xn)-processes leading to the formation of ^{90}Nb, ^{89m}Nb and ^{89}Nb. The values for ^{90}Nb describe the cumulative formation cross section. Error bars are also shown. The solid curve is an eye-guide through our data. A few available points for ^{90}Nb from the literature [9] are also shown.

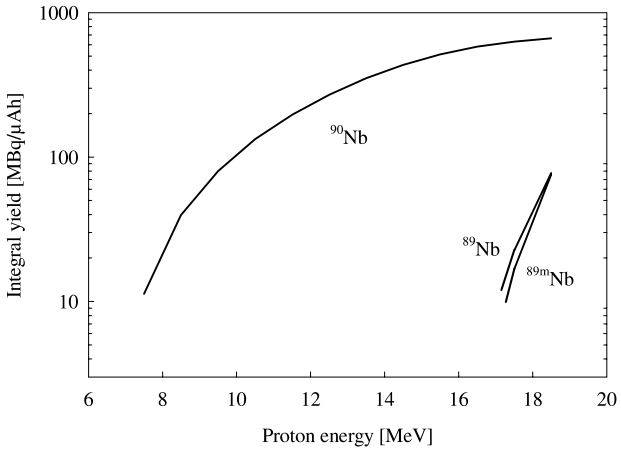

Fig. 2. Thick target yields of ^{90}Nb, ^{89m}Nb and ^{89}Nb calculated from the excitation functions measured in this work (cf. Fig. 1).

Theoretical integral yields

The differential and integral yields of the niobium radioisotopes at EOB formed in the two nuclear processes, viz ^{90}Zr(p, n)^{90}Nb and ^{90}Zr(p, $2n$)^{89m,89}Nb, were calculated from the experimentally measured excitation functions (Fig. 1) and the stopping powers, assuming a 1 h irradiation at 1 μA. The stopping powers were calculated on the basis of the Bethe-Bloch equation which, using the formalism of Williamson *et al*. [19], has been transformed to a computer program "STACK" at Jülich. The integral yields are given in Fig. 2. Up to about 17 MeV, ^{90}Nb is the only product. The formation of ^{89m,89}Nb becomes relevant only at proton energies > 17 MeV.

From the excitation function (Fig. 1) and the yield curve (Fig. 2) it is evident that the optimum energy range for the production of ^{90}Nb is $E_p = 17 \rightarrow 7$ MeV. For this energy range the integral yield amounts to 600 MBq ^{90}Nb/μA h. At a somewhat higher proton energy, *e.g.* 19 MeV, some ^{89m,89}Nb will also be formed. However, because of the longer half-life of ^{90}Nb, the ratio of the product nuclide ^{90}Nb to the radionuclidic impurties ^{89m,89}Nb would become better with extended irradiation times.

Experimental thick target yields

Using three ^{nat}Zr foils of 250 μm thickness each, thick target yields were determined experimentally. In Table 3 the experimental values are given together with the calculated ones. There is a good agreement between the experimental and calculated yield data of ^{90}Nb for proton energies < 15 MeV, *i.e.* when only the (p, n)-reaction occurs. For E_p > 15 MeV the experimental values are slightly higher due to some contribution of the ^{91}Zr(p, $2n$)^{90}Nb-process to the formation of ^{90}Nb. The last two columns give the calculated yields of ^{90}Nb if 100% enriched ^{90}Zr in metallic form or as $^{90}ZrO_2$ would be used. Evidently, those yields are higher.

Impurities

The radionuclidic impurities of some concern in the production of ^{90}Nb from highly enriched ^{90}Zr are the Nb isotopes 89m and 89, and their Zr and Y decay products ^{89m}Zr ($T_{1/2}$ = 4.2 min), ^{89}Zr ($T_{1/2}$ = 78.4 h) and ^{89m}Y ($T_{1/2}$ = 16 s), resulting from the ^{90}Zr(p, $2n$)-reaction at high incident projectile energies. The production of these impurities can be avoided by limiting the incident proton energy to below the threshold energy of the (p, $2n$)-reaction, however, with a somewhat lower ^{90}Nb yield. Because of the relatively short half-lives of ^{89m,89}Nb as compared to ^{90}Nb, the level of these impurities decreases with time; consequently a simultaneous production of these short-lived isotopes can be tolerated to a certain extent. In addition to the above mentioned impurities some other isotopic Nb-impurities like ^{91m,92m,96}Nb may also occur. Their levels depend on the isotopic abundances of ^{91,92,96}Zr in the enriched ^{90}Zr sample. Additionally, ^{90}Zr(p, α)^{87}Y and ^{90}Zr(p, pn)^{89}Zr reactions may occur. These are, however, of no great significance since Zr and Y can be chemically separated from the radioniobium.

Table 3. Experimental and calculated thick target yields of ^{90}Nb for a 30 min irradiation of ^{nat}Zr with a 1 μA proton beam and respective calculated yields for ^{nat}Zr and 100% enriched ^{90}Zr-metal as well as $^{90}ZrO_2$.

Foil No.	E_p [MeV]	Yield of ^{90}Nb [MBq/μA h] from various targets			
		^{nat}Zr (exp.)	^{nat}Zr (cal.) *via* ^{90}Zr(p, n)-reaction	^{90}Zr-metal (cal.) (100% enriched)	$^{90}ZrO_2$ (cal.) (100% enriched)
1	17.6 → 15.0	128	89	173	110
2	15.0 → 11.9	120	123	239	152
3	11.9 → 8.1	82	95	184	118
2 + 3	15.0 → 8.1	202	218	423	270
1 + 2 + 3	17.6 → 8.1	330	307	596	380

Table 4. Measured levels of radioniobium impurities ($1\,a > T_{1/2} > 10\,min$) after a 30 min irradiation of ^{nat}Zr as percent of total radioniobium activity for different proton energy ranges (values refer to 4 h after EOB).

Foil No.	E_p [MeV]	^{89m}Nb [a] (1.1 h)	^{89}Nb [a] (2.0 h)	^{90}Nb (14.6 h)	^{91m}Nb (62 d)	^{92m}Nb (10.2 d)	^{95m}Nb (3.61 d)	^{95}Nb (35 d)	^{96}Nb (23.4 h)
1+2+3	17.6 → 8.1	1.28	0.33	96.15	0.10	0.92	0.34	0.12	0.76
2+3	15.0 → 8.1	–	–	96.91	0.10	1.42	0.36	0.12	1.10
3	11.9 → 8.1	–	–	94.96	0.08	2.39	0.33	0.09	2.15

a: Calculated values

As far as the production of ^{90}Nb from ^{nat}Zr is concerned, the typical composition of radioniobium found after a 30 min irradiation of ^{nat}Zr is given in Table 4. The values were obtained *via* a γ-ray spectrometric analysis of all the radioisotopes at 4 h post EOB and are given as % of the total niobium activity.

A period of 4 h after EOB was chosen as a realistic time with respect to the separation of ^{90}Nb from a Zr target and the synthesis of a potential ^{90}Nb-radiopharmaceutical for nuclear medical application. As can be concluded from Table 4, the ^{90}Nb activity is almost constant at about 95%–97% over the investigated energy range of $E_p = 17.6 \rightarrow 8.1$ MeV. The levels of the activities of ^{92m}Nb and ^{96}Nb are not very high and the 95% purity of ^{90}Nb may be acceptable for some (animal) nuclear medical applications. However, it is recommended that the radiation dose from those three impurities should be estimated prior to large scale production and application in humans of ^{90}Nb produced from ^{nat}Zr. With 100% enriched ^{90}Zr targets, however, the yield of ^{90}Nb in the energy ranges of $E_p = 17.6 \rightarrow 8.1$ MeV and $E_p = 15.0 \rightarrow 8.1$ MeV could be increased by a factor of 1.81 and 1.94, respectively, and the contributions of Nb-radioisotopes other than ^{90}Nb could be diminished by one to two orders of magnitude.

Conclusion

The results of the cross section measurements clearly indicate that ^{90}Nb can be produced with batch activities of the order of 10 GBq and in high radionuclidic purity by means of the (p, n)-process on highly enriched ^{90}Zr at a small cyclotron providing maximum proton energies of about 17 MeV. Sufficient quantities of ^{90}Nb can also be produced using ^{nat}Zr as target material; the radionuclidic purity, however, would then be about 96%, the main contaminant being 10.2 d ^{92m}Nb.

Acknowledgment. The authors wish to thank Prof. H. H. Coenen for supporting this study and the crew of the Compact Cyclotron CV 28 at the Forschungszentrum Jülich GmbH for the irradiations.

References

1. Busse, S., Brockmann, J., Rösch, F.: Effecitve radiochemical separation of no-carrier-added $^{90g/95g}$Nb from macroscopic amounts of ^{nat}Zr. J. Labelled Cpd. Radiopharm **42**, Suppl. 1, 906–908 (1999).
2. Busse, S., Brockmann, J., Rösch, F.: [^{90g}Nb]DFO-Succinyl-(D)-Phe^1-Octreotide: First radiolabeling experiments of DFO-Succinyl-(D)Phe^1-Octreotide (SDZ 216-927) with analogous no-carrier-added ^{95g}Nb and investigation of its *in vitro* stability. J. Labelled Cpd. Radiopharm **42**, Suppl. 1, 300–302 (1999).
3. Kundu, D. N., Pool, M. L.: Columbium 90. Phys. Rev. **75**, 1690 (1949).
4. Butement, F. D. S., Qaim, S. M.: New radioisotopes of niobium and molybdenum I. J. Inorg. Nucl. Chem. **26**, 1481 (1964).
5. Mercader, R. C., Caracoche, M. C., Mocoroa, A. B.: Excitation functions for the production of ^{90}Nb and ^{88}Y by irradiation of zirconium with deuterons. Z. Physik **255**, 103 (1972).
6. Wasilevsky, C., Dos Santos, F., Herreros Usher, O., Nassiff, S. J.: Excitation functions and thick target yields for deuteron induced reactions on zirconium. Radiochem. Radioanalyt. Lett. **32**, 127 (1978).
7. Gonchar, A. V., Kondratev, S. N., Lobach, Yu. N., Nevskii, S. V., Skylyarenko, V. D., Tokarevskii, V. V.: Formation of long-lived radionuclides by irradiation of zirconium with deuterons. Atomnaja Energija **75**, 205 (1993).
8. Smend, F., Weirauch, W., Schmidt-Ott, W.-D., Flammersfeld, A.: Cross sections and isomeric ratios for the reactions ^{89}Y$(\alpha, 3n)^{90g}$Nb and ^{89}Y$(\alpha, 3n)^{90m}$Nb. Z. Physik **207**, 28 (1967).
9. Kondratev, S. N., Kuzmenko, V. A., Lobach, Yu. N., Prokopenko, V. S., Sklyarenko, V. D., Tokarevskii, V. V.: Radionuclide production cross sections up to 70 MeV by interaction of protons with zirconium nuclides. Atomnaja Energija **71**, 325 (1991).
10. Michel, R., Bodemann, R., Busemann, H., Daunke, R., Gloris, M., Lange, H.-J., Klug, B., Krins, A., Leya, I., Lüpke, M., Neumann, S., Reinhardt, H., Schnatz-Büttgen, M., Herpers, U., Schiekel, Th., Sudbrock, F., Homqvist, B., Condé, H., Malmborg, P., Suter, M., Dittrich-Hannen, B., Kubik, P.-W., Synal, H.-A., Filges, D.: Cross sections for the production of residual nuclides by low- and medium-energy protons from the target elements C, N, O, Mg, Al, Si, Ca, Ti, V, Mn, Fe, Co, Ni, Cu, Sr, Y, Zr, Nb, Ba and Au. Nucl. Instrum. Methods B **129**, 153 (1997).
11. Weinreich, R., Schult, O., Stöcklin, G.: Production of ^{123}I *via* the ^{127}I$(d, 6n)^{123}$Xe$(\beta^+$,EC$)^{123}$I process. Int. J. Appl. Radiat. Isot. **25**, 353 (1974).
12. Qaim, S. M., Stöcklin, G., Weinreich, R.: Excitation functions for the formation of neutron deficient isotopes of bromine and krypton *via* high-energy deuteron induced reactions on bromine: Production of ^{77}Br, ^{76}Br and ^{79}Kr. Int. J. Appl. Radiat. Isot. **28**, 947 (1977).
13. Rösch, F., Qaim, S. M., Stöcklin, G.: Nuclear data relevant to the production of the positron emitting radioisotope ^{86}Y *via* the ^{86}Sr(p, n)- and ^{nat}Rb$(^3$He,$xn)$-processes. Radiochim. Acta **61**, 1 (1993).
14. Piel, H., Qaim, S. M., Stöcklin, G.: Excitation functions of (p, xn)-reactions on natNi and highly enriched ^{62}Ni: Possibility of production of medically important radioisotope ^{62}Cu at a small cyclotron. Radiochim. Acta **57**, 1 (1992).
15. Tárkányi, F., Takács, S., Gul, K., Hermanne, A., Mustafa, M. G., Nortier, M., Oblozinský, P., Qaim, S. M., Scholten, B., Shubin, Yu. N., Zhuang Youxiang: Beam monitor reactions. In: *Charged Particle Cross Section Database for Medical Radioisotope Production*. IAEA-TECDOC-1211 (2001) pp. 47–150.
16. Browne, E., Firestone, R. B.: *Table of Radioactive Isotopes*. (Shirley, V. S. Ed.) John Wiley and Sons, New York (1986).
17. Kastleiner, S., Qaim, S. M., Coenen, H. H.: Excitation functions of proton induced reactions on enriched ^{70}Zn and ^{85}Rb for the production of medically important radioisotopes ^{67}Cu and ^{83}Sr, 5th Int. Conf. on Nuclear and Radiochemistry, Pontresina, Switzerland, September 2000, PSI Villigen, Extended Abstracts Vol. 2 (2000) p. 645.
18. Rösch, F., Qaim, S. M.: Nuclear data relevant to the production of the positron emitting technetium isotope ^{94m}Tc *via* the ^{94}Mo(p, n)-reaction. Radiochim. Acta **62**, 115 (1993); Erratum **75**, 227 (1996).
19. Williamson, C. F., Boujot, J. P., Picard, J.: Tables of range and stopping power of chemical elements for charged particles of energy 0.5 to 500 MeV. Report CEA-R 3042 (1966).